

Winter temperatures over the Korean Peninsula and East Asia: development of a new index and its application to seasonal forecast

Seon Tae Kim¹  · Soo-Jin Sohn¹ · Jong-Seong Kug²

Received: 8 June 2016 / Accepted: 13 October 2016 / Published online: 21 October 2016
© Springer-Verlag Berlin Heidelberg 2016

Abstract This study proposes a new index for monitoring and predicting winter temperatures of the Korean Peninsula based on the dominant atmospheric winter teleconnection patterns. The utilization of this index is further extended to the East Asian Winter Monsoon (EAWM) index because the new index is found to well represent the main feature of the EAWM circulation. Among the teleconnection patterns, the East Atlantic (EA) and Western Pacific (WP) patterns are found to be most strongly correlated with winter temperatures via their partial association with changes in sea level pressure (SLP) around the Korean Peninsula, i.e., the EA and WP patterns are associated with SLP variation over the Siberian High region and the Kuroshio extension region to the east of Japan, respectively. On the basis of this relationship, the two regions representing the northwest-to-southeast SLP gradients are determined to define the new index. It is found that the new index can represent the Korean winter temperatures consistently well regardless of their considerable decadal changes. When compared with the existing SLP-based EAWM indices, the new index shows the best performance in delineating winter air temperatures, not only in the Korean Peninsula but also in the entire East Asian region. We also assess the prediction skill of the new index with seasonal coupled forecast models of the APEC Climate Center of Korea and its capability to predict winter temperatures. This assessment shows that the new index has potential for operationally predicting and

monitoring winter temperatures in Korea and the whole of East Asia.

Keywords Teleconnection · EAWM · Winter temperature prediction

1 Introduction

Because extreme events such as cold surges have societal and economic impacts, there have been substantial efforts to predict and understand the winter climate in the Korean Peninsula and East Asia (Ding and Krishnamurti 1987; Boyle and Chen 1987; Min et al. 2015). Variability of the winter climate in the Korean Peninsula has been understood primarily within the context of the East Asian Winter Monsoon (EAWM) circulation system. Variation in the EAWM system is related to thermal contrasts between the Asian land mass and the adjacent oceans (e.g., Zhang et al. 1997; Trenberth et al. 2006). The land–ocean thermal contrasts are associated with the sea level pressure (SLP) gradient between the Siberian High over the northeastern part of Eurasia and the Aleutian Low over the North Pacific Ocean (Gong et al. 2001; Wu and Wang 2002; Jhun and Lee 2004; Chen et al. 2005; Takaya and Nakamura 2005; Wu et al. 2006). In recognizing this, many studies have made significant attempts to reveal the dynamics involved in SLP gradient changes.

Many studies have linked the East Asian winter climate to the atmospheric teleconnection patterns. These patterns are the preferred modes of low-frequency variability in the Northern Hemisphere (NH) and are characterized by a horizontal scale of the planetary waves with multiple centers of action. These teleconnection patterns can influence the weather and climate in East Asia and the Korean Peninsula

✉ Seon Tae Kim
seontae.kim@apcc21.org

¹ Climate Prediction Department, APEC Climate Center, Busan, South Korea

² School of Environmental Science and Engineering, Pohang University of Science and Technology, Pohang, South Korea

Table 1 Existing SLP-based EAWM indices and their definition

EAWM index	SLP area-averaging regions	References
ChanLi04	(30°–55°N, 100°–120°E)–(30°–55°N, 150°–170°E)	Chan and Li (2004)
Gong01	(40°–60°N, 70°–120°E)	Gong et al. (2001)
Guo94	(10°–60°N, 110°E)–(10°–60°N, 160°E)	Guo (1994)
Shi96*	(20°–50°N, 110°E)–(20°–50°N, 160°E)	Shi (1996)
WangChen14*	{2 × (40°–60°N, 70°–120°E)–(30°–50°N, 140°E–170°W)–(20°S–10°N, 110°–160°E)}/2	Wang and Chen (2014)
Wang09*	(40°–70°N, 110°E)–(40°–70°N, 160°E)	Wang et al. (2009)
WuWang02*	(20°–70°N, 110°E)–(20°–70°N, 160°E)	Wu and Wang (2002)
XuJi65	(30°–40°N, 100°–120°E)–(30°–40°N, 130°–140°E)	Xu and Ji (1965)

* Indicates that the definition of the index uses the normalized SLPs

(Wallace and Gutzler 1981; Horel and Wallace 1982; Lau and Lau 1984; Nakamura et al. 1987; Barnston and Livezey 1987; Chen et al. 2005) because such patterns can affect the variation in the intensity of the Siberian High and the Aleutian Low (Cohen et al. 2001; Gong et al. 2001).

Among the teleconnection patterns, the Arctic Oscillation (AO; Thompson and Wallace 1998) affects the intensity of the Siberian High (Gong et al. 2001; Gong and Ho 2004; Kug et al. 2015). The variation of the Siberian High, which is associated with the AO, can affect the occurrence frequency of cold surge events (e.g., Jeong and Ho 2005; Park et al. 2011). Park and Ahn (2015) showed that the AO influence can vary depending on the phase of the Western Pacific (WP) teleconnection pattern, which is most significantly correlated with the East Asian winter temperatures among the dominant teleconnection patterns over the Pacific Ocean sector. They argued that the relationship between the East Asian temperature and the AO is clear only when the AO is in phase with the WP pattern. The WP pattern has two anomaly centers, one near Kamchatka (50°N–60°N, 160°E–170°W) and the other over the North Pacific Ocean (20°N–30°N, 160°W–130°E); these centers are signed opposite to one another and are known to influence the intensity of the Aleutian Low (Hsu and Wallace 1985; Linkin and Nigam 2008).

In addition to the AO and WP teleconnection patterns, many prominent atmospheric teleconnection patterns in the NH winter have been investigated since Walker and Bliss (1932) recognized the North Atlantic Oscillation (NAO) and North Pacific Oscillation (Wallace and Gutzler 1981; Barnston and Livezey 1987; Nakamura et al. 1987; Linkin and Nigam 2008; Wang and Zhang 2014), including the Pacific/North American pattern (PNA), the East Atlantic pattern (EA), and the Eurasian pattern (EU). In particular, the EU teleconnection pattern [distinguished as EU type-1 and EU type-2 patterns in Barnston and Livezey (1987), whereas the EU types are referred to as the East Atlantic/Western Russia (EA/WR) and the Scandinavia (SCA) pattern, respectively, on the National Centers for

Environmental Prediction (NCEP) Climate Prediction Center (CPC) website] is characterized by east–west wave trains and has three action centers over the Eurasian continents. Because the EU pattern can be significantly correlated with the intensity of the Siberian High, the pattern affects the East Asian winter on monthly and daily time scales (Gong et al. 2001; Takaya and Nakamura 2005; Sung et al. 2009; Sohn et al. 2011; Wang and Zhang 2014).

However, although the variation in the Siberian High intensity can be associated with a wave train originating from the Atlantic Ocean, the influence of the EA teleconnection pattern on the Korean and East Asian winter temperatures is not well-known. The EA pattern is the second mode of low-frequency variability over the North Atlantic Ocean and has a north–south dipole of anomaly centers crossing the North Atlantic from east to west. Furthermore, only a few studies have been performed on the role of the teleconnection patterns in varying the Korean winter temperatures. Therefore, investigating the relationship between the winter teleconnection patterns and the winter temperatures over Korea is necessary. On the basis of this relationship, this study proposes a useful index for representing winter temperatures over the Korean Peninsula in Sect. 3, and further shows change in the proposed new index is related to the EAWM circulation.

Many EAWM indices have been developed based on SLP gradients between the Eurasian continents and Pacific Ocean (Wang and Chen 2010, 2014), as listed in Table 1. Although the existing EAWM indices can delineate the key features of the EAWM-related circulations, differences were found to exist in the performance of these indices in representing variation of the East Asian winter temperatures, in particular, extreme cold and warm winters (Wang and Chen 2010, 2014). Furthermore, there are no studies comparing the EAWM indices regarding the representation of Korean winter temperature variation. Therefore, it will be very meaningful to compare the ability of the SLP-based EAWM indices, including the proposed new index, to represent the Korean winter temperatures, because they can be

Table 2 Five seasonal prediction coupled climate models used in this study, including references and model institutes

Model	Institute	References
CMCC	Euro-Mediterranean Center on Climate Change	Alessandri et al. (2010)
CM3	Meteorological Service of Canada	Merryfield et al. (2013)
CM4		
NCEP	NCEP/NOAA/CPC	Saha et al. (2014)
POAMA	Bureau of Meteorology	Lim et al. (2012)

utilized for monitoring and predicting the Korean winter climates.

Because the new index should have reasonable prediction capabilities even if the index reliably describes the change in the observed winter temperature, we also assess its capability and usability for Korean and East Asian winter temperature prediction with seasonal forecast coupled models in Sect. 6.

2 Datasets and methods

2.1 Observed datasets

For observed land surface air temperatures, we use a station observation-based global land monthly surface air temperature dataset (Fan and van den Dool 2008), which was developed at the NCEP CPC. This dataset combines station datasets collected from the Global Historical Climatology Network version 2 and the Climate Anomaly Monitoring System (GHCN + CAMS) gridded at a resolution of 0.5° latitude \times 0.5° longitude. Observed atmospheric variables such as SLP, geopotential height at 500 hPa, zonal wind at 200 hPa, and near-surface wind are taken from the NCEP–National Center for Atmospheric Research (NCAR) reanalysis I (Kalnay et al. 1996). The land surface air temperatures and the NCEP–NCAR reanalysis datasets are used over the period from December 1950 to February 2015.

Indices for the NH atmospheric teleconnection patterns are downloaded, and detailed information about these patterns can be obtained from the CPC website (<http://www.cpc.ncep.noaa.gov/data/teledoc/telecontents.shtml>). To describe briefly, the NH teleconnection patterns (e.g., the PNA, NAO, WP, EA, SCA, EA/WR patterns) and their associated indices are obtained by performing Rotated Principal Component Analysis (Barnston and Livezey 1987) of the monthly mean standardized 500 hPa geopotential height anomalies taken from the NCEP–NCAR reanalysis project. The AO index is obtained from the Empirical Orthogonal Function analysis of monthly mean 1000 hPa height anomalies.

We use the December–January–February (DJF) average for indicating the winter climate in the Korean Peninsula

and the entire East Asian region. Therefore, all analyses performed in the following sections use atmospheric variables and climate indices averaged over the DJF season. Here, the winter period calendar years are denoted using the year in which December fell, e.g., the winter of year 1997 covers December 1997–February 1998. Anomalous variables are obtained by subtracting their DJF climatological averages.

2.2 Hindcast datasets of APCC MME system and index-based predictions

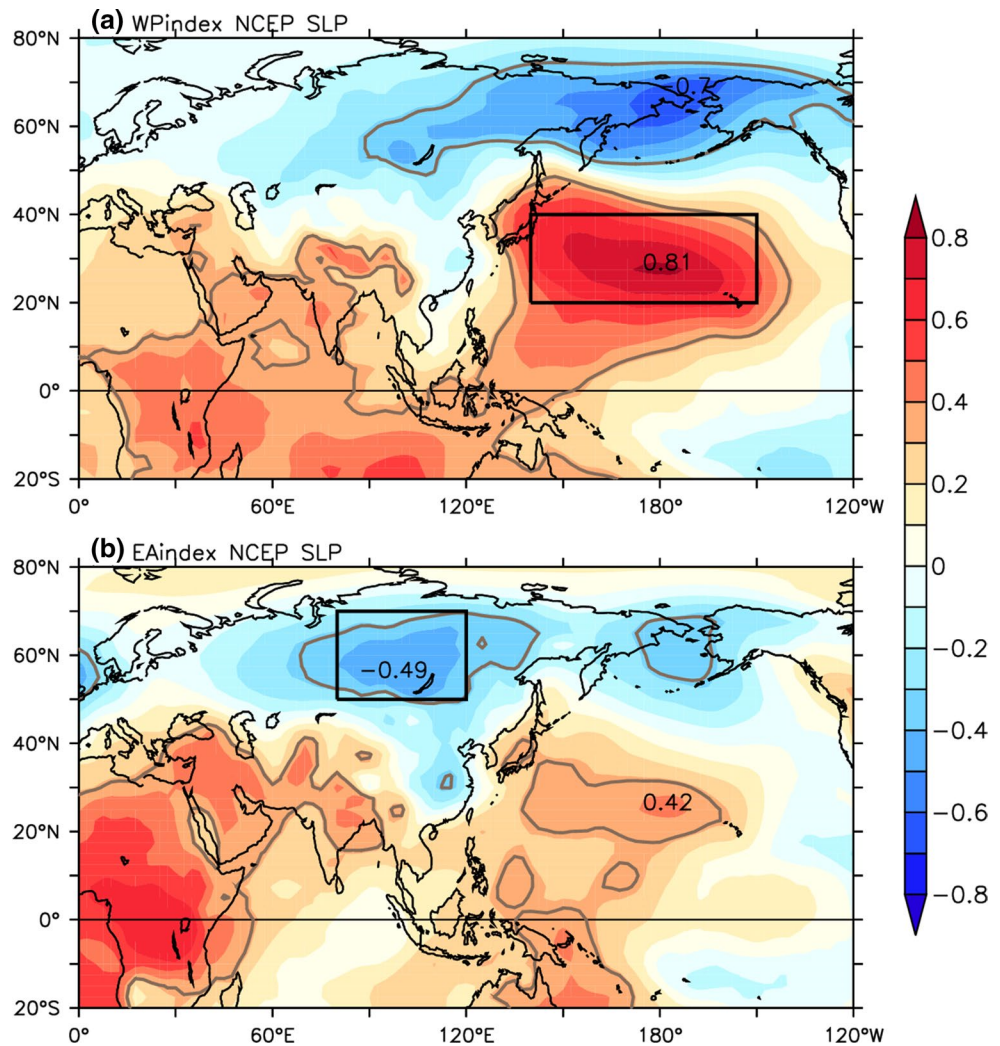
We use hindcast datasets from five coupled seasonal forecast models (shown in Table 2) to investigate the prediction skill of the new index, which will be proposed in Sect. 3 and used for predicting the winter surface air temperatures of the Korean Peninsula and the entire East Asian region. These models are being used for seasonal forecasting at the APEC Climate Center (APCC), Korea. The seasonal forecast models were initialized in November, and we analyze surface air temperatures and SLPs during the subsequent winter season (i.e., the DJF average), which indicates a 1-month lead prediction. The hindcast period is from December 1983 to February 2006.

Two measures, such as temporal correlation coefficient (TCC) and anomaly pattern correlation coefficient (ACC), are used for verifying the historical prediction skills on the new index and its associated winter temperatures. For the skill in predicting the new index itself, we computed the TCC between the predicted and observed index. In order to check the capability of the new index in predicting the spatial patterns of winter temperatures, we perform ACC analysis between the observed and predicted values over the Korean Peninsula (123°E – 130°E , 33°N – 40°N) and East Asian (100°E – 145°E , 20°N – 50°N) regions. The predicted spatial patterns of the winter temperature anomalies in each year can be obtained directly from the raw multi-model ensemble (MME) of the APCC seasonal forecast models. Also, the predicted patterns can be provided by the regression relationship between the simulated index and MME winter temperatures at each grid point. The raw MME output without any correction, which is considered as raw MME predictions, and the corrected MME output with

Table 3 Correlation coefficients between the winter temperature averaged over the Korean Peninsula (KorT; 123°E–130°E, 33°N–40°N) and the NH winter atmospheric teleconnection indices (including AO)

Climate indices	PNA	NAO	WP	EA	SCA (EU1)	EA/WR (EU2)	AO
KorT	−0.08	0.18	0.59	0.50	−0.18	0.40	0.40

Fig. 1 Spatial patterns of correlation coefficients of winter (December–January–February, DJF) SLPs with **a** WP and **b** EA teleconnection indices. Significant correlation coefficients ($r = 0.32$) at the 99 % level according to a two-tailed student's t-test are indicated with gray contour lines. Black boxes denote the regions for defining the new index. Local positive and negative maxima of the correlation coefficients are also shown



the simulated index (as a predictor), which is regarded as index-based predictions, are compared.

3 New index

In order to identify the NH winter atmospheric teleconnection patterns that dominate changes in the Korean winter temperature, correlation coefficients between the winter temperature averaged over the Korean Peninsula (123°E–130°E, 33°N–40°N) and the indices associated with the teleconnection patterns are calculated, as shown

in Table 3. The WP and EA indices are found to have the strongest correlations ($r = 0.59$ and 0.50 , respectively) with the Korean winter temperatures.

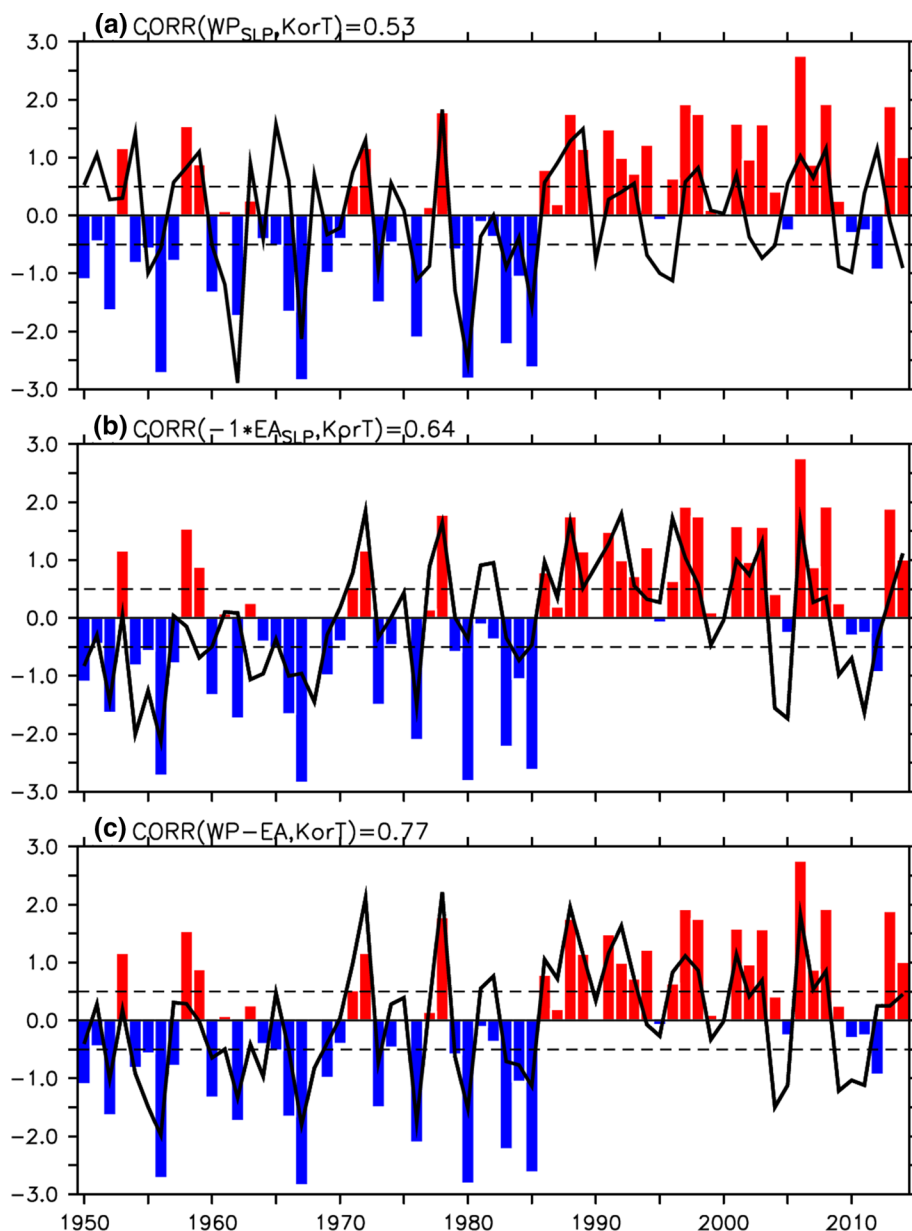
Because teleconnection patterns reflect large scale change in atmospheric pressure and circulation anomalies that spans broad geographical regions, the patterns would be responsible for change in the SLP patterns around the Korean Peninsula. Therefore, we investigate the correlation coefficient patterns of the DJF SLP with the WP and EA indices, as shown in Fig. 1. Both patterns are found to be related to change in SLPs around the Korean Peninsula. In other words, when concentrating on land and ocean regions

around the Korean Peninsula, the WP has the highest correlation ($r = 0.81$, Fig. 1a) with the SLPs over the Kuroshio extension region to the east of Japan. In contrast, the EA pattern is most strongly correlated ($r = -0.49$, Fig. 1b) with the SLPs over the Siberian High region. On the basis of this relationship, we determine the two regions indicated by black boxes in Fig. 1. The SLPs averaged over the boxed regions are similar to those that were identified earlier for describing the East Asian winter climate. The EA-related boxed region ($80^{\circ}\text{E}-120^{\circ}\text{E}$, $50^{\circ}\text{N}-70^{\circ}\text{N}$) is similar to the region of the Siberian High intensity index (e.g., Li and Yang 2010; Jeong et al. 2011), which has been frequently used for monitoring the winter temperatures over East Asia, including the Korean Peninsula (e.g., Gong and Ho

2002; Chang and Lu 2012). The WP-related boxed region ($140^{\circ}\text{E}-150^{\circ}\text{W}$, $20^{\circ}\text{N}-40^{\circ}\text{N}$) resides at the southwestern edge of the Aleutian Low and encompasses the Kuroshio extension region over which SLP variation is known to be important in determining the Korean winter climate (Son et al. 2013).

Here, for representing the Korean winter temperatures, we explore the possibility of using the SLPs averaged over both the EA- and WP-related boxed regions, which are hereafter referred to as the EA SLP index and the WP SLP index, respectively. For comparison, we have multiplied the SLPs averaged over the EA-related region by -1.0 to define the EA SLP index. From the time series of the Korean Peninsula temperature anomalies and the EA and

Fig. 2 Time series of seasonal (DJF) mean SLP (black line) averaged over **a** $140^{\circ}\text{E}-150^{\circ}\text{W}$, $20^{\circ}\text{N}-40^{\circ}\text{N}$ and **b** $80^{\circ}\text{E}-120^{\circ}\text{E}$, $50^{\circ}\text{N}-70^{\circ}\text{N}$, which are related to the WP SLP and EA SLP regions, respectively, and **c** time series of difference (black line) between SLPs averaged over the regions in **a** and **b**, which is the definition of the new index. Times series of the DJF-mean temperatures ($^{\circ}\text{C}$) averaged over the Korean Peninsula (colored bars; red bars for warm temperatures and blue bars for cold temperatures) are also superimposed in each panel. The SLP indices are normalized using their standard deviation. Dashed lines denote thresholds for classifying extreme warm or cold winter years and a high or low index



WP SLP indices shown in Fig. 2, it is identified that the EA and WP SLP indices are strongly correlated with the winter temperature anomaly of Korea ($r = 0.64$ and 0.53 , respectively). However, if we focus on the extreme cold and warm winters, which are defined when the temperature anomaly is below -0.5 °C and above $+0.5$ °C, respectively, following Wang and Chen (2014), and their correspondence with the low and high EA and WP SLP indices, some extreme cold or warm winters cannot be explained by the EA SLP index or WP SLP index alone. Here, the high and low index is distinguished based on a threshold of ± 0.5 standard deviations (STD) of each index. For example, the 1962, 1980, and 2008 extreme winters only can be captured by the WP SLP index, whereas the extreme winters in 1984 and 2014 only can be represented by the EA SLP index. The results indicate that both the WP and EA SLP indices can make up for each other in terms of the discrepancy in predicting winter temperatures of the Korean Peninsula. Furthermore, the relative strength of SLPs over the EA- and WP-related regions may govern the cold advection from the Siberian regions southeastward to the Korean Peninsula. Therefore, we propose a new index for capturing the variation of the Korean winter temperatures; this is defined as the difference between SLPs averaged over the WP- and EA-related boxed regions, as follows.

$$\text{New index} = \text{WP SLP}(140^{\circ}\text{E}-150^{\circ}\text{W}, 20^{\circ}\text{N}-40^{\circ}\text{N}) \\ - \text{EA SLP}(80^{\circ}\text{E}-120^{\circ}\text{E}, 50^{\circ}\text{N}-70^{\circ}\text{N}).$$

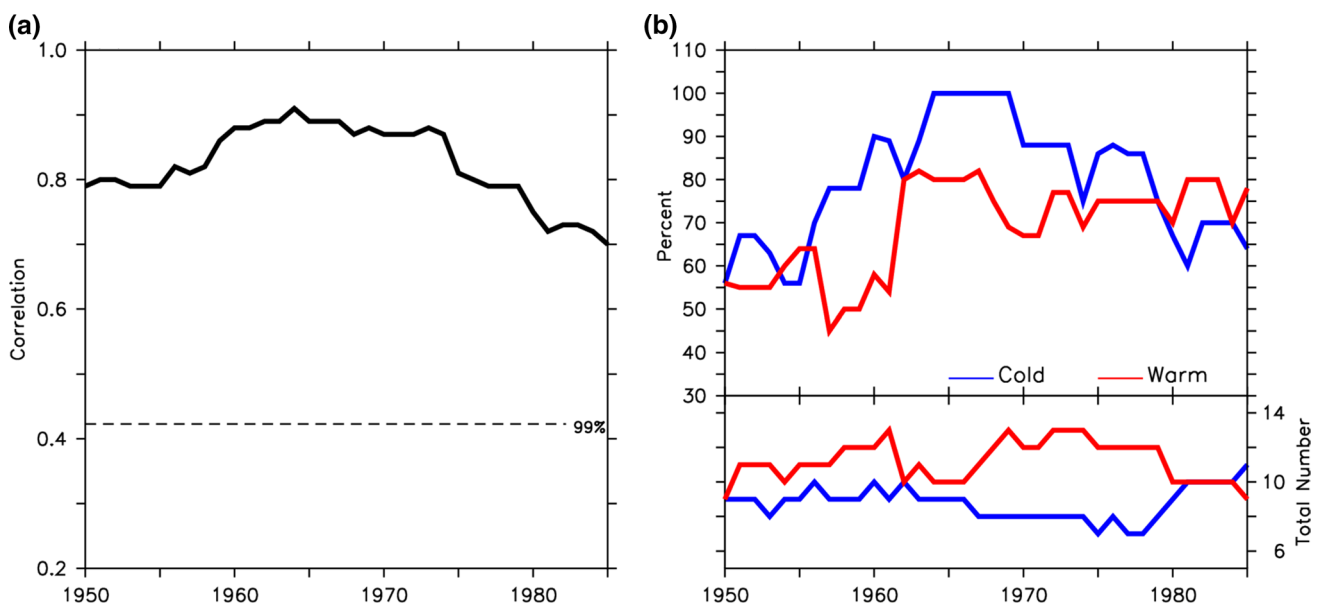


Fig. 3 **a** Correlation coefficients between the new index and winter temperature over the Korean Peninsula, and **b** the number (percentage) of extreme cold (blue lines) and warm (red lines) winters corresponding to low and high new index, respectively. The correlation coefficients and percentages are computed over 30-year running peri-

ods from 1950 to 2014. In **a** the 99 % significant correlation coefficient is indicated with a dashed line and in **b** the total number of extreme cold (blue lines) and warm (red lines) winters are also displayed. The x-axis denotes the start year of the 30-year running periods

As a result, the new index can obtain a better representation of the Korean Peninsula winter temperatures. The correlation coefficient increases significantly to 0.77 (Fig. 2c). Furthermore, the new index is correlated significantly (at the 99 % level according to a two-tailed student's t test) with both WP ($r = 0.65$) and EA ($r = 0.50$) teleconnection patterns, which indicates that the new index can reflect well the influence of both teleconnection patterns on the Korean winter temperatures. When considering extreme winters, there is considerable improvement in representing the extreme cold winters with the new index. The low new index (< -0.5 STD) corresponds to 75 % (15 out of 20 winters) of the extreme cold Korean winters, whereas the EA SLP index only can capture about 55 % of the extreme cold winters and WP SLP index can capture about 45 %. As for the extreme warm winters (corresponding to index that is larger than $+0.5$ STD), the new index, and EA and WP SLP indices produce similar result; each can capture 71, 63, and 71 % of total 24 extreme warm winters.

As shown in Fig. 2, one may suggest that the Korean winter temperatures have been experiencing considerable decadal changes and the relationship between the new index and local temperature could be changed over the inter-decadal timescales. In order to investigate whether the new index has consistent performance over the different periods, we compute the correlation coefficients between the Korean winter air temperatures and the new index (Fig. 3a) computed over 30-year periods running forward

one year from 1950 to 2014. This indicates that the new index maintains a strong correlation with the Korean winter temperatures throughout the running periods. The maximum and minimum correlation coefficients are 0.91 and 0.70, respectively. Furthermore, in terms of the number of extreme cold or warm winters over the Korean Peninsula captured by the new index (Fig. 3b), the new index can represent more than 60 % of extreme winters over most of the running periods. The new index can generally depict the extreme cold winters better than the extreme warm cases, which is beneficial if we consider the hazardous impact of extreme cold winters on the national socio-economic activity. These results imply that the new index can represent the Korean temperature consistently well to some extent in spite of the considerable decadal changes.

4 The new index and EAWM circulation

Here, we investigate whether the intensity of the new index can explain the characteristics of the EAWM circulation and can thus be utilized for predicting the winter temperatures of the entire East Asia, including Japan and East China, beyond Korea. Figure 4 shows the regression patterns of the SLPs, the zonal winds at 200 hPa, and the 500 hPa geopotential heights with the new index. Some typical characteristics of the winter monsoon circulation, such as the East Asian jet stream, the 500-hPa trough, and their associated surface northwesterly winds, can be identified (e.g., Jhun and Lee 2004; Li and Yang 2010; Hu et al. 2015). Here, the regression patterns illustrate the lower and upper tropospheric circulation patterns during the weak EAWM because a positive or high value of the new index indicates a weak EAWM. Therefore, a low (high) new index, representing a strong (weak) EAWM, is linked to the enhanced (weakened) East Asian westerly jet stream to the south of the Korean Peninsula and Japan (Fig. 4a). The trough in the middle troposphere is strengthened (weakened) when the index is low or negative (high or positive), as shown in Fig. 4b. These lower and upper tropospheric patterns contribute to a change in the northwesterly winds blowing from the Siberian High region to the East Asian countries (Fig. 4c). Therefore, the figure indicates that the new index can represent the main components of the EAWM system and can be further utilized for monitoring the East Asian winter climate, including not only the Korean Peninsula, but also the East China and Japan (as shown in Sect. 5).

In addition, El Niño-like surface winds (i.e., westerly anomalies) reside over the central equatorial Pacific, which highlights the possible link between El Niño and the EAWM represented with the new index; this is

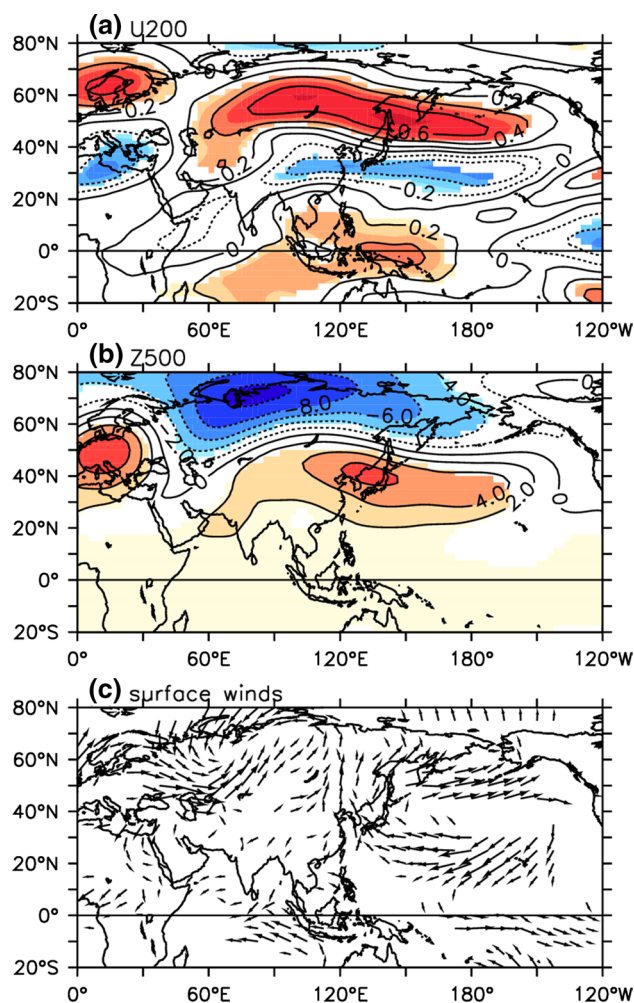


Fig. 4 Spatial regression patterns of **a** zonal winds at 200 hPa, **b** 500 hPa geopotential heights, and **c** near-surface winds with the new index. Regression coefficients that are significant at the 95 % level according to a two-tailed student's t-test are shaded in **(a)** and **(b)**. The regressed surface winds with 95 % significance are only shown in **(c)**

consistent with previous studies showing the close relationship between El Niño-Southern Oscillation (ENSO) and EAWM (e.g., Zhang et al. 1997; Jiang et al. 2013). However, the correlation coefficient ($r = 0.32$) between the new index and the DJF-averaged Niño3.4 index is not that strong, although it is significant at 99 % level according to a two-tailed student's t-test. The Niño3.4 index is the sea surface temperature (SST) anomaly averaged over 120°W–170°W and 5°S–5°N. The SST is taken from the NOAA Extended Reconstructed SST (ERSST) v3b (Smith et al. 2008). This may affect the prediction skill of the new index in coupled forecast models; this is further discussed in Sect. 6.

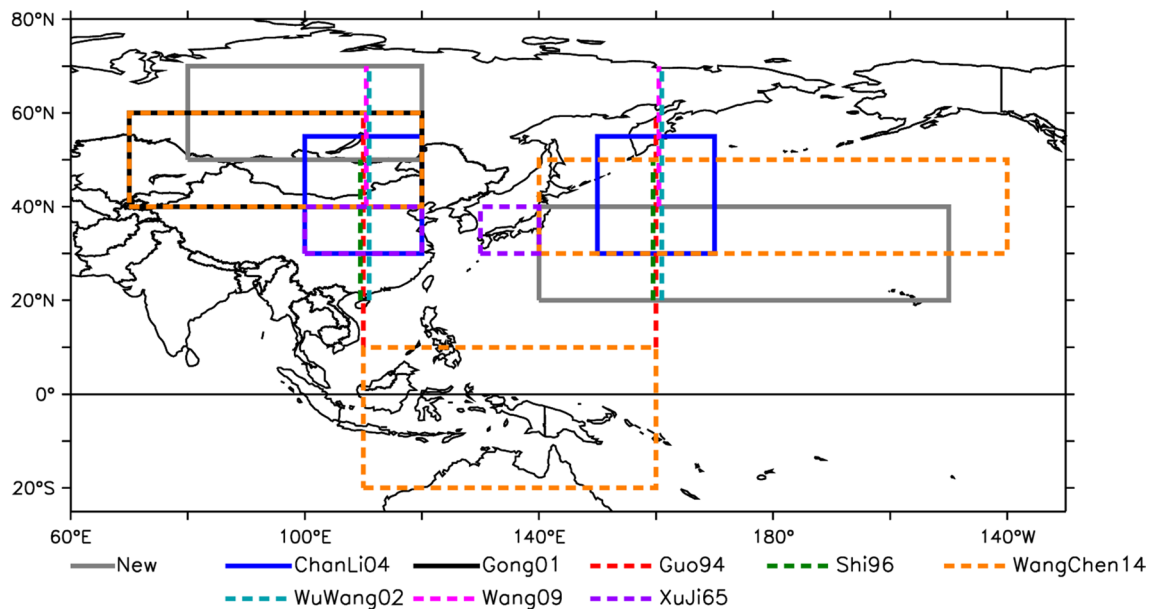


Fig. 5 Illustration of the *boxed regions* for defining the existing SLP-based EAWM index, as listed in Table 1, and the new index

5 The new index and existing SLP-based EAWM indices

In this section, we compare the ability of the new index to represent the Korean and East Asian winter temperatures with that of the existing SLP-based EAWM indices listed in Table 1. Figure 5 illustrates the SLP averaging regions used in the definitions of the EAWM indices. Although the EAWM indices define the SLP regions and reflect the land–ocean thermal contrasts, the averaging regions are different from one another. Methods proposed by Guo (1994, hereafter Guo94), Shi (1996, Shi96), Wu and Wang (2002, WuWang02), and Wang et al. (2009, Wang09) use SLPs averaged along a fixed longitude (110°E) and within different latitude ranges. In contrast, as is done for the new index, indices proposed by Chan and Li (2004, ChanLi04), Gong et al. (2001, Gong01), Wang and Chen (2014, WangChen14), and Xu and Ji (1965, XuJi65) are defined by the area-averaging boxed regions, e.g., WangChen14 proposed an EAWM index considering not only the east–west contrast of the SLP over the Siberian region with the Aleutian SLP but also the north–south contrast of the Siberian SLP with the SLP over the maritime continents.

From Fig. 6, which displays the spatial pattern of correlation coefficients between surface temperatures over East Asia and the EAWM indices (including the new index), it is identified that the EAWM indices show differing levels of performance in representing the surface air temperature variation over the Korean Peninsula as well as the entire East Asian region. Here, the existing SLP-based EAWM indices have been multiplied by -1.0 for comparison.

Overall the new index has the best performance among the SLP-based EAWM indices at capturing change in the winter temperature (Fig. 6a). The correlation coefficients that are significant at the 99 % level ($r > 0.32$) cover the entire East China, Japan, and Korean Peninsula region, and they also extend to regions of Mongolia. In particular, the strongest correlation coefficients ($r > 0.7$) reside over the Korean Peninsula. The winter temperatures over the coastal regions of Southeastern China correlate strongly ($r > 0.5$) with the new index. Other EAWM indices have significant correlations with the winter temperatures averaged over East Asia at a 99 % level (except for the XuJi65). The WangChen14, WuWang02, and Guo95 indices have correlation coefficients with the winter temperature averaged over the Korean Peninsula that are greater than 0.6. Further strong correlation coefficients for those indices are centered over the Korean Peninsula. This indicates that these EAWM indices are also usable for the Korean winter temperature representation.

6 Potential of the new index in seasonal forecasting

This section investigates the prediction skill of the new index and the WangChen14 index in coupled seasonal forecast models and evaluates their potential in predicting winter surface air temperatures over the Korean Peninsula and the entire East Asian region based on both indices as predictors. Here, we only choose the WangChen14 index for the comparison because other than the new index,

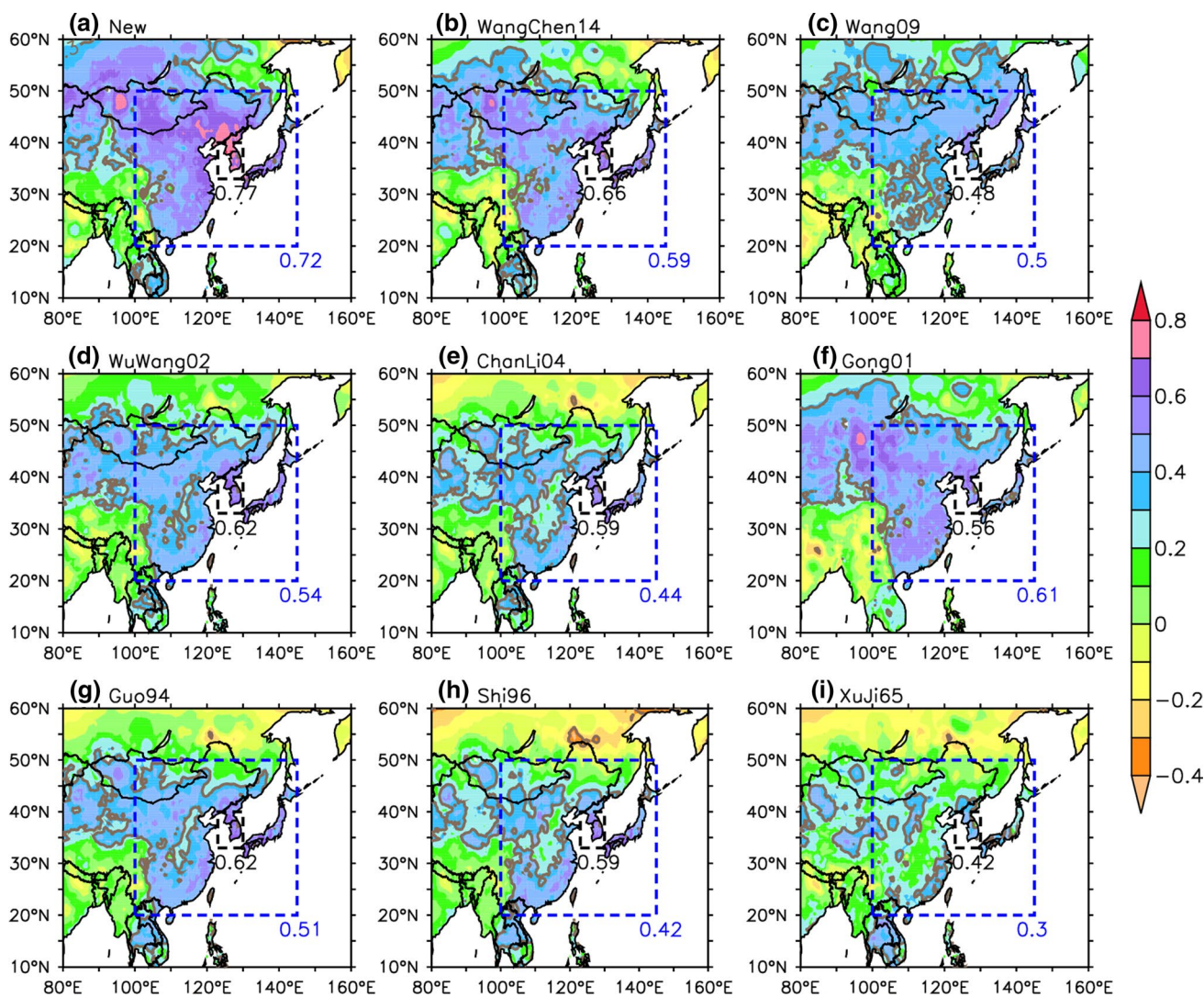


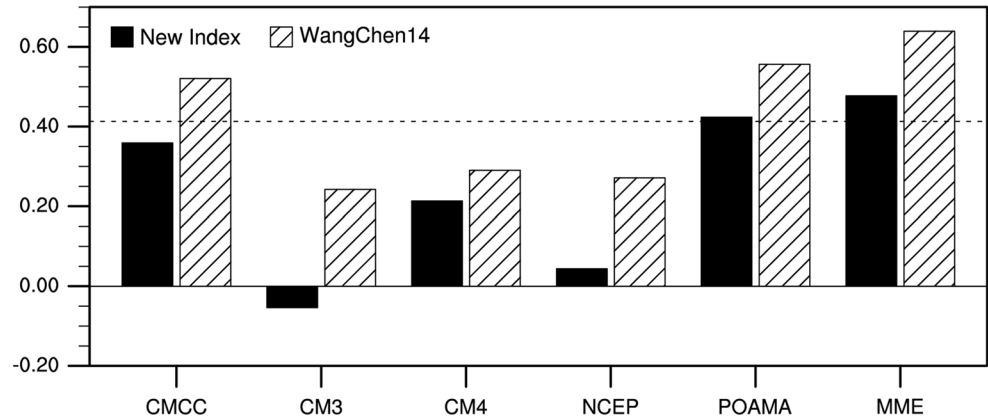
Fig. 6 Spatial patterns of correlation coefficients between SLP-based EAWM indices and winter temperatures over the East Asian region: **a** new, **b** Wang and Chen (2014), **c** Wang et al. (2009), **d** Wu and Wang (2002), **e** Chan and Li (2004), **f** Gong et al. (2001), **g** Guo (1994), **h** Shi (1996), and **i** Xu and Ji (1965). Significant correlation coefficients ($r = 0.32$) at the 99 % level according to a two-tailed student's

t-test are indicated with *gray contour lines*. Correlation coefficients with temperatures averaged over the East Asia (20°N–50°N, 100°E–145°E; *blue dashed box*) and Korean Peninsula (123°E–130°E, 33°N–40°N; *black dashed box*) regions are shown. Before computing the correlation coefficients, all the EAWM indices, except the new index, are multiplied by -1.0

this is the index that shows the best performance among the SLP-based EAWM indices. Figure 7 displays TCCs between the observed and predicted indices from the hindcast simulations of the coupled models. Overall, the skill of the WangChen14 index forecast is better in all the models used in this study and also in their MME mean forecast using a simple composite method. This may be because in the observations, the WangChen14 index is more strongly correlated with the Niño3.4 index ($r = 0.48$), which is an important source of the predictability of the winter climate including the EAWM in coupled forecast models (Peng et al. 2009; Kim et al. 2012; Jiang et al. 2013), than the new index ($r = 0.32$). In addition, the higher correlation

between the WangChen14 index and the Niño3.4 index can be inferred from the definition of the EAWM index, which is based on three domains: the western Eurasia, the North Pacific, and the tropical western Pacific (see Fig. 5). In particular, climate variables in the tropical western Pacific region are not only more strongly related to ENSO events but are also more predictable than those in the other regions. Consequently, the relatively high prediction skill score of the WangChen14 index may be associated with this predictability source. In contrast, because the new index considers the domains over mid-latitudes, the skill score of the new index prediction cannot achieve that of the WangChen14 index in most models. Nonetheless,

Fig. 7 TCCs between the observed and model simulated DJF-mean EAWM indices for the period 1982–2004. Retrospective forecast models are listed in Table 2. *Solid bars* denote the new index and *hatched bars* denote WangChen14 index. *Dashed lines* indicate the threshold for the 95 % significance level



the POAMA model provides a capable prediction for both new and WangChen14 indices, with significant TCCs at the 95 % level. When we use the MME prediction, we can

expect improved prediction capabilities for both indices; this has been suggested by previous studies (e.g., Kirtman 2003; Jin et al. 2008). This result indicates that we can

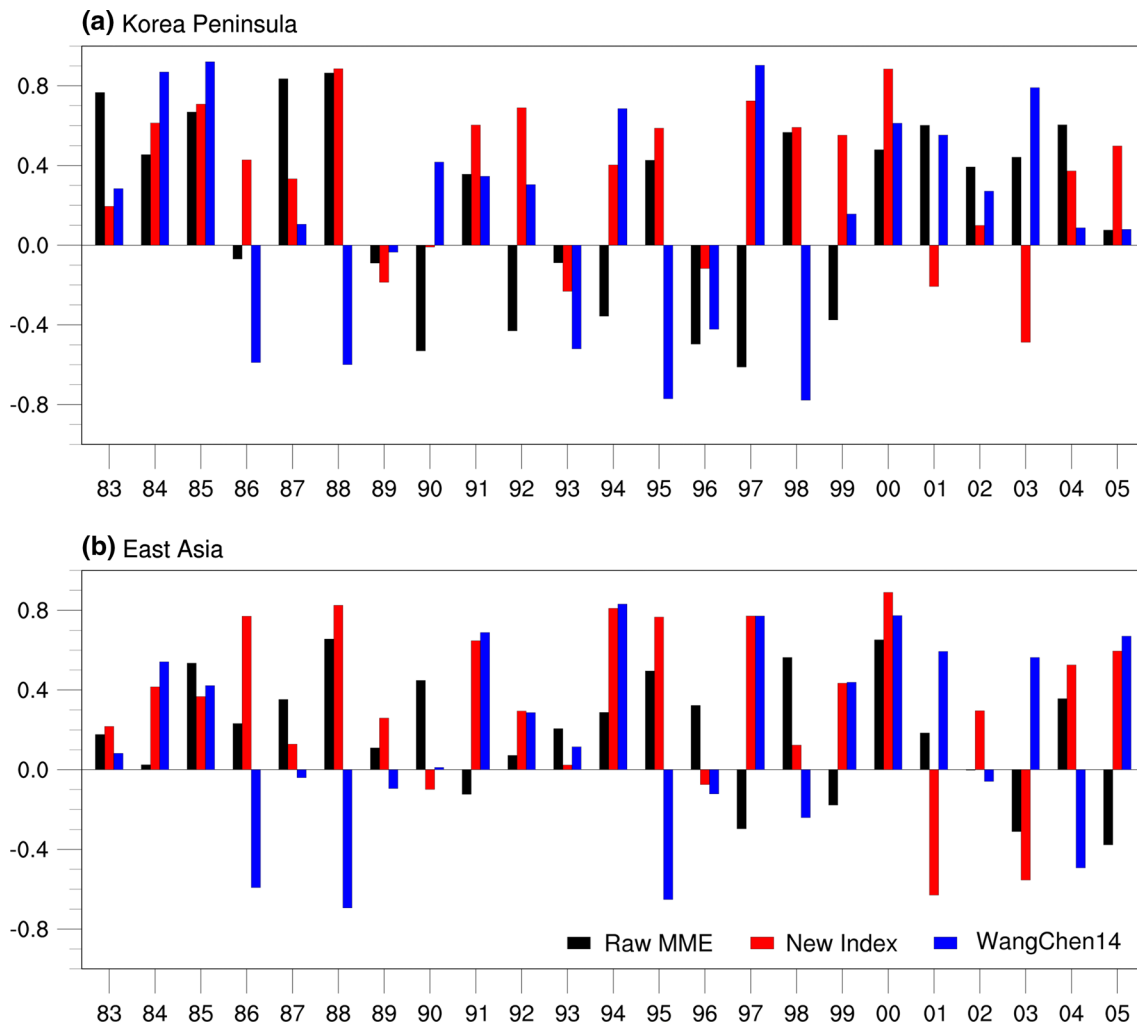


Fig. 8 Time series of the ACCs between the observed and model simulated DJF-mean temperature anomalies in **a** the Korean Peninsula and **b** East Asian regions. *Black bars* denote the direct model

output from the raw MME. *Red and blue bars* denote the index-based temperature predictions with the new index and WangChen14 index, respectively

dynamically predict the new index, which can in turn be utilized for predicting both the Korean and East Asian winter temperatures, by employing the coupled forecast models, particularly the APCC MME system.

Because the new index is designed to capture the winter temperature variation of the Korean Peninsula and East Asia, we also investigate the potential for using the EAWM indices simulated in the seasonal forecast coupled models to better predict the winter temperatures. Figure 8 shows the ACCs between the observed and predicted winter air temperature anomalies, which are obtained directly from the raw MME and linear regression relations (i.e., index-based predictions, see Sect. 2) computed over the Korean Peninsula and the East Asian region. The spatial similarities between the observed and predicted patterns appears to quite fluctuate from year to year, and there is a big inconsistency in three time series of the ACCs from the raw MME-based predictions and index-based predictions. For winter temperatures in the Korean Peninsula and entire East Asia, the new index has a better overall capability at predicting the spatial patterns of the winter surface air temperatures. Particularly, the new index-based predictions have more winter years with the ACC that is greater than 0.5, compared with other methods (i.e., raw MME-based predictions and the WangChen14 index-based predictions).

Furthermore, the winter temperatures for both Korean and entire East Asian regions from raw MME-and WangChen14 index-based predictions show much more tendency to have opposite spatial patterns against observations (i.e., negative ACCs) than those from the new index-based predictions.

Better prediction skills with the new index can be identified when the ACCs were averaged over the whole years, extreme cold and warm years, and normal years as shown in Fig. 9. The mean ACC over the hindcast periods (23 years, Fig. 9a) from the new index is 0.34 for the Korean winter temperatures, which is greater than the ACCs from the raw MME-based (ACC = 0.19) and the WangChen14 index-based (ACC = 0.16) predictions. For the East Asian winter temperatures (Fig. 9e), the new index-based prediction did achieve as much capable predictions regarding the spatial patterns as they did for the Korean winter temperatures. The new index (ACC = 0.34) provides much better prediction capability than the raw MME (ACC = 0.19) and the WangChen14 index (ACC = 0.17). When only considering extreme cold winter years, the new index-based predictions have more advantages in capturing the temperature variation over the Korean and East Asian regions. The ACC scores from the new index-based predictions are larger than 0.45. In temperature predictions for the normal and warm winter years, the new index does not provide strong ACC

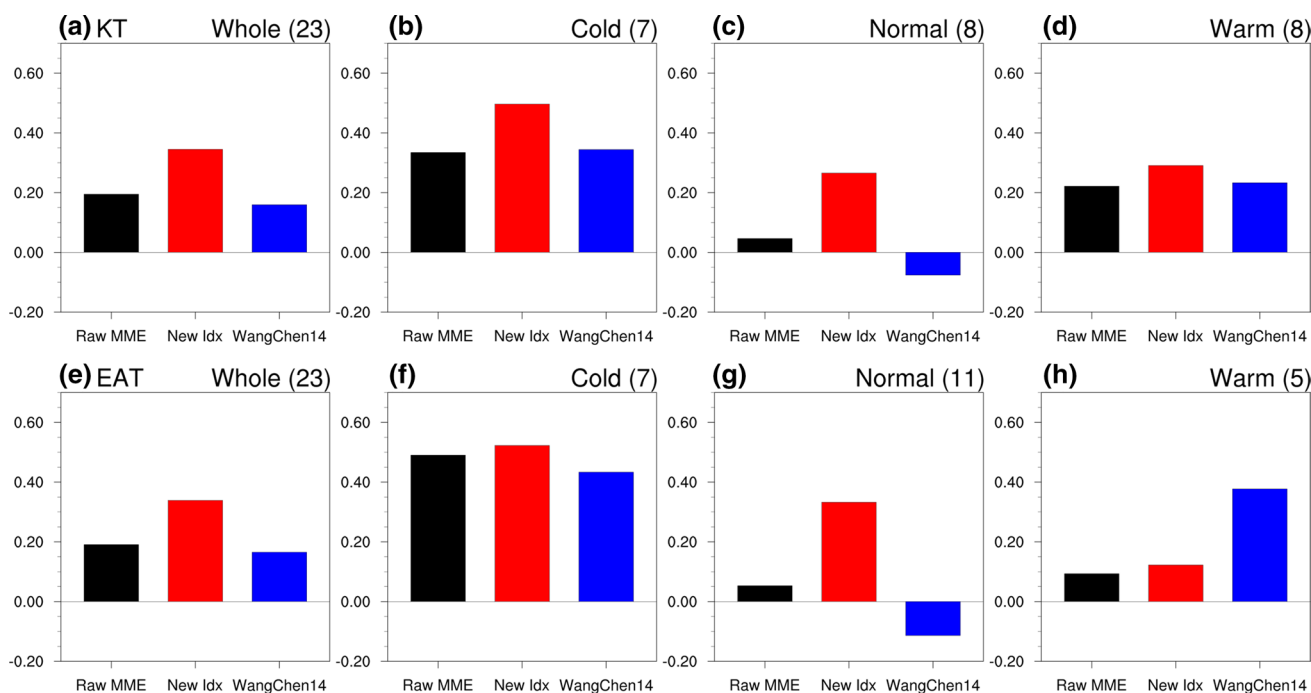


Fig. 9 ACCs (presented in Fig. 8) between the observed and model simulated winter temperature anomalies in **a–d** the Korean Peninsula and **e–h** East Asian regions averaged over **a, e** whole, **b, f** extreme cold, **c, g** normal, and **d, h** extreme warm years. The extreme cold and warm winters selected are listed in Table 4, and the rest are nor-

mal years. The numbers of the selected winter years are provided in parentheses at the upper right of each panel. Black bars denote the direct model output from the raw MME. Red and blue bars denote the index-based temperature predictions with the new index and WangChen14 index, respectively

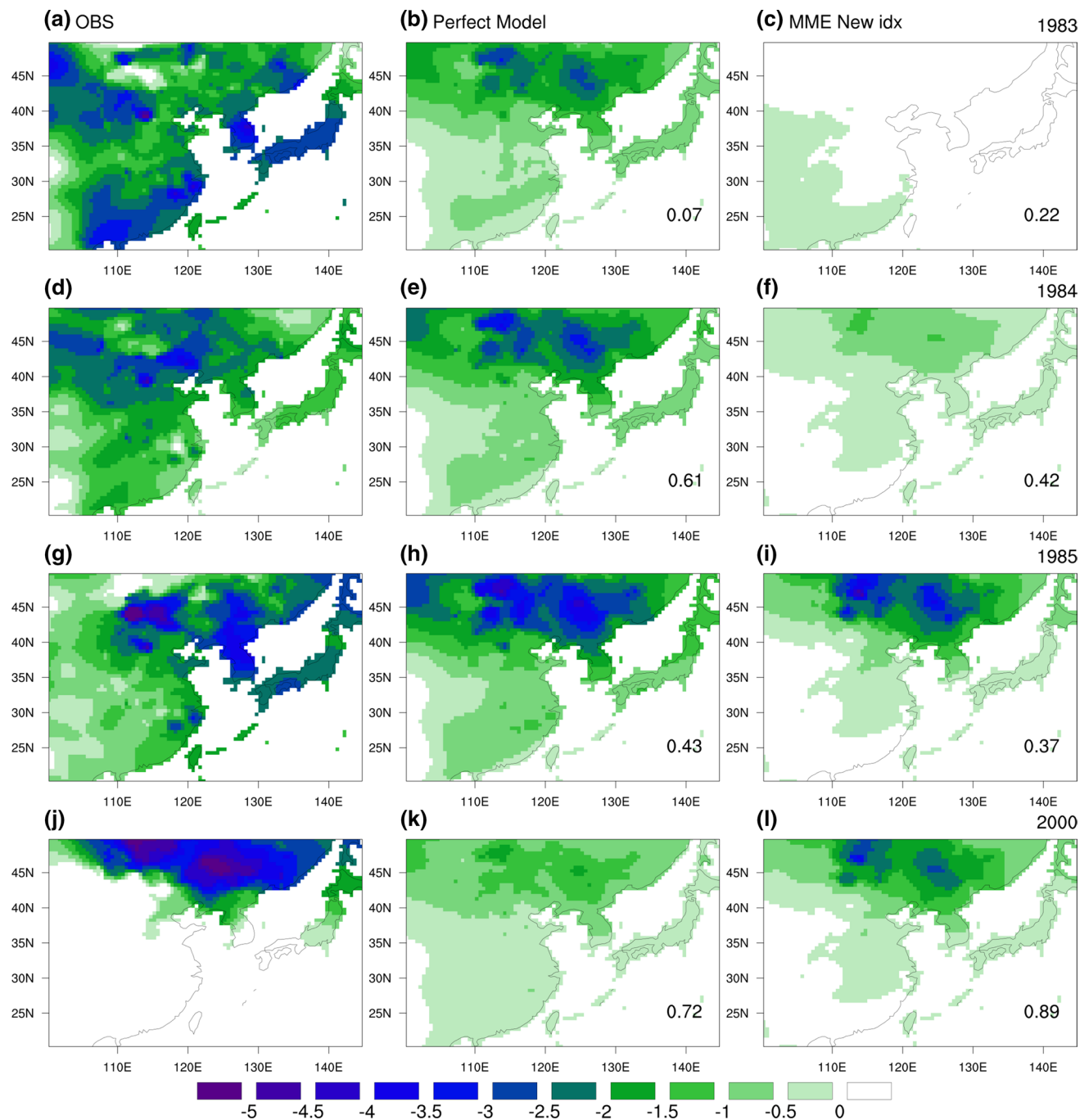


Fig. 10 Spatial patterns of winter temperature anomalies from **a, d, g, j** observations, and index-based predictions using **b, e, h, k** observations (i.e., perfect model) and **c, f, i, l** MME outputs for the extreme cold years in both Korean and entire East Asian regions (see

also Table 4) **a–c** 1983, **d–f** 1984, **g–i** 1985, and **j–l** 2000. The ACCs between the observed and predicted temperatures in the East Asian regions are shown in *bottom right* of (**b, c, e, g, h, i, k, l**) each panel. See main text for details

skill as much as for the cold winter years. The lower skills of the raw MME-based predictions for the Korean Peninsula and East Asian temperatures are mainly due to the fact that the East Asian winter climate is difficult to predict in the current frame of dynamical seasonal prediction system and there is low potential predictability of the temperature

in the mid latitudes (Sohn et al. 2011). In other words, there exists the upper limit of prediction level at which a state-of-the-art coupled prediction system can predict winter temperatures.

Figure 10 shows the spatial distribution of temperatures during extreme cold winters from observations,

Table 4 Lists of extreme cold and warm winters from 1983 to 2005

	Extreme cold winters	Extreme warm winters
KorT	1983 (−2.78), 1984 (−1.61), 1985 (−3.18), 1990 (−0.55), 1995 (−0.63), 2000 (−0.58), 2005 (−0.81)	1988 (1.20), 1989 (0.59), 1991 (0.93), 1994 (0.67), 1997 (1.36), 1998 (1.19), 2001 (1.02), 2003 (1.02)
EAT	1983 (−1.96), 1984 (−1.57), 1985 (−1.51), 1987 (−0.56), 1999 (−0.80), 2000 (−0.55), 2004 (−0.89)	1990 (0.53), 1997 (0.74), 1998 (1.40), 2001 (1.55), 2003 (0.86)

Those winters are identified from temperature anomaly based on climatological land temperatures over the period 1983–2005

The area averaged temperature anomaly (°C) over the Korean Peninsula (KorT) and entire East Asia (EAT) are indicated in parentheses

perfect model, and new index-based prediction. We selected extreme cold winter years when both observed temperatures averaged over the Korean and entire East Asian regions are less than -0.5 °C (see Table 4). The “perfect model” is constructed with a regression equation based on the observed new index, not model simulated, as predictor to predict the East Asian temperature variation. Here, the perfect model assumption is that dynamical model can perfectly predict the observed new index, and thus the perfect model provides the upper limit of the new index-based prediction. For 1983, the severe cold anomalies are observed over the southeast China, South Korea, and southern Japanese Archipelagos. However, the perfect model and the new index-based winter temperature predictions do not capture those patterns. The cold anomalies are probably attributed to other factors, for example, originating from the tropics (e.g., Wang et al. 2000) or the Arctic (e.g., Kug et al. 2015). For other extreme cold winters (i.e., 1984, 1985, 2000), observed cold anomalies are present to the north of the Korean Peninsula and the new index-based prediction can predict the cold anomalies. Furthermore, the new index-based predictions have ACC skill scores that are very comparable to those of the perfect model.

In conclusion, the above results imply that the new index is more effective at foreseeing winter temperature variations over the East Asian region, as well as the Korean Peninsula, than the direct model output (i.e., raw MME based-predictions).

7 Summary and discussion

This study proposed a new index for monitoring and predicting winter temperatures over the Korean Peninsula and further over the entire East Asian region. As a first step, we found the atmospheric teleconnection patterns during the NH winter that are correlated strongly with the Korean winter temperatures. As a second step, we identified the atmospheric circulation patterns, namely SLP patterns, around the Korean Peninsula that are associated with the strongly correlated teleconnection patterns; i.e.,

among the teleconnection patterns, it was found that both EA and WP teleconnection patterns are most strongly related to the change in winter temperatures. The EA and WP patterns are related to SLP variations over both the Siberian High region and the Kuroshio extension region to the east of Japan, respectively. In fact, these two pressure systems dominate the winter climate over East Asia, including the Korean Peninsula. Because the SLP gradients control the intensity of surface winds blowing into the Korean Peninsula from the Siberian regions (which could cause cold air advection), the two predominant regions representing the northwest-to-southeast SLP gradients were selected for the new index definition. It was identified that the new index can represent the Korean winter temperatures consistently well regardless of their considerable decadal changes.

Change in the new index was found to be associated with the EAWM circulation. When compared with the previously existing SLP-based EAWM indices, the new index showed the best performance in representing winter temperature variation, not only in the Korean Peninsula, but also in the entire East Asian region.

Because the skill of the new index forecast in coupled seasonal forecast models is important for a good EAWM index (Li and Yang 2010), the current status of the prediction skill of the new index as well as its potential for seasonal forecasting with climate models (i.e., APCC MME forecast system) were investigated. The APCC MME system was found to provide reliable forecast capabilities with the new index. When performing index-based predictions, the new index provides the prediction skills for the winter temperatures over the Korean Peninsula and East Asia that are better than the raw MME-based predictions and comparable to the perfect model predictions. Therefore, we concluded that it would be beneficial to utilize the new index as a predictor for monitoring and predicting the Korean and East Asian winter climates.

In this study, we identified the role of the WP and EA teleconnection patterns in varying the Korean winter temperatures. However, we did not reveal the factors associated with the variation in these teleconnection patterns, which would require extensive analysis. There should be

subsequent studies because the related dynamics would be important for more capable prediction and monitoring of the East Asian climate.

Acknowledgments Authors acknowledge that the GHCN Gridded V2 data are provided by the NOAA/OAR/ESRL PSD, Boulder, Colorado, USA, from their website at <http://www.esrl.noaa.gov/psd/>. The authors also acknowledge that the APCC Multi Model Ensemble (MME) Producing Centers for making their data available for analysis and the APEC Climate Center for collecting and archiving them and for organizing APCC MME prediction. Authors thank anonymous reviewers for constructive comments. This research was supported by the APEC Climate Center.

References

- Alessandri A, Borrelli A, Masina S, Di Pietro P, Carril AF, Cherchi A, Gualdi S, Navarra A (2010) The INGV-CMCC seasonal prediction system: improved ocean initial conditions. *Mon Weather Rev* 138:2930–2952
- Barnston AG, Livezey RE (1987) Classification, seasonality and persistence of low-frequency atmospheric circulation patterns. *Mon Weather Rev* 115:1083–1126
- Boyle JS, Chen TJ (1987) Synoptic aspects of the winter-time east Asian monsoon. In: Chang CP, Krishnamurti TN (eds) *Monsoon meteorology*. Oxford University Press, Oxford, pp 125–160
- Chan JCL, Li CY (2004) The East Asia winter monsoon. In: Chang CP (ed) *East Asian Monsoon*. World Scientific, Singapore, pp 54–106
- Chang C-P, Lu M-M (2012) Intraseasonal predictability of Siberian high and East Asian Winter Monsoon and its interdecadal variability. *J Clim* 25:1773–1778
- Chen W, Yang S, Huang RH (2005) Relationship between stationary planetary wave activity and the East Asian winter monsoon. *J Geophys Res* 110:D14110
- Cohen J, Saito K, Entekhabi D (2001) The role of the Siberian high in northern hemisphere climate variability. *Geophys Res Lett* 28:299–302
- Ding Y, Krishnamurti TN (1987) Heat budget of the Siberian high and the winter monsoon. *Mon Weather Rev* 115:2428–2449
- Fan Y, van den Dool H (2008) A global monthly land surface air temperature analysis for 1948–present. *J Geophys Res* 113:D01103
- Gong D-Y, Ho C-H (2002) Siberian high and climate change over middle to high latitude Asia. *Theoret Appl Climatol* 72:1–9
- Gong D-Y, Ho C-H (2004) Intra-seasonal variability of wintertime temperature over East Asia. *Int J Climatol* 24:131–144
- Gong D-Y, Wang S-W, Zhu J-H (2001) East Asian winter monsoon and Arctic oscillation. *Geophys Res Lett* 28:2073–2076
- Guo QY (1994) Relationship between the variations of East Asian winter monsoon and temperature anomalies in China (in Chinese). *Quat J Appl Meteor* 5:218–225
- Horel JD, Wallace JM (1982) Planetary-scale atmospheric phenomena associated with the Southern Oscillation. *Mon Weather Rev* 109:813–829
- Hsu H-H, Wallace JM (1985) Vertical structure of wintertime teleconnection patterns. *J Atmos Sci* 42:1693–1710
- Hu C, Yang S, Wu Q (2015) An optimal index for measuring the effect of East Asian winter monsoon on China winter temperature. *Clim Dyn* 45:2571–2589
- Jeong J-H, Ho C-H (2005) Changes in occurrence of cold surges over east Asia in association with Arctic Oscillation. *Geophys Res Lett* 32:L14704
- Jeong J-H, Ou T, Linderholm HW, Kim B-M, Kim S-J, Kug J-S, Chen D (2011) Recent recovery of the Siberian High intensity. *J Geophys Res Atmos* 116:D23102
- Jhun J-G, Lee E-J (2004) A new east Asian winter monsoon index and associated characteristics of the winter monsoon. *J Clim* 17:711–726
- Jiang X, Yang S, Li Y, Kumar A, Wang W, Gao Z (2013) Dynamical prediction of the East Asian winter monsoon by the NCEP Climate Forecast System. *J Geophys Res Atmos* 118:1312–1328
- Jin EK et al (2008) Current status of ENSO prediction skill in coupled ocean–atmosphere models. *Clim Dyn* 31:647–664
- Kalnay E et al (1996) The NCEP/NCAR 40-year reanalysis project. *Bull Am Meteorol Soc* 77:437–471
- Kim H-M, Webster PJ, Curry JA (2012) Seasonal prediction skill of ECMWF System 4 and NCEP CFSv2 retrospective forecast for the Northern Hemisphere Winter. *Clim Dyn* 39:2957–2973
- Kirtman BP (2003) The COLA anomaly coupled model: ensemble ENSO prediction. *Mon Weather Rev* 131:2324–2341
- Kug J-S, Jeong J-H, Jang Y-S, Kim B-M, Folland CK, Min S-K, Son S-W (2015) Two distinct influences of Arctic warming on cold winters over North America and East Asia. *Nat Geosci* 8:759–762
- Lau N-C, Lau K-M (1984) The structure and energetics of midlatitude disturbances accompanying cold-air outbreaks over East Asia. *Mon Weather Rev* 112:1309–1327
- Li Y, Yang S (2010) A dynamical index for the East Asian winter monsoon. *J Clim* 23:4255–4262
- Lim EP, Hendon HH, Langford S, Alves O (2012) Improvements in POAMA2 for the prediction of major climate drivers and south eastern Australian rainfall. CAWCR Tech. Rep. No. 051. <http://www.cawcr.gov.au/publications/technicalreports.php>
- Linkin ME, Nigam S (2008) The north pacific oscillation–west pacific teleconnection pattern: mature-phase structure and winter impacts. *J Clim* 21:1979–1997
- Merryfield WJ et al (2013) The Canadian seasonal to interannual prediction system. Part I: models and initialization. *Mon Weather Rev* 141:2910–2945
- Min S-K et al (2015) Changes in weather and climate extremes over Korea and possible causes: a review. *Asia-Pac J Atmos Sci* 51:103–121
- Nakamura H, Tanaka M, Wallace JM (1987) Horizontal structure and energetics of Northern Hemisphere wintertime teleconnection patterns. *J Atmos Sci* 44:3377–3391
- Park H-J, Ahn J-B (2015) Combined effect of the Arctic oscillation and the Western Pacific pattern on East Asia winter temperature. *Clim Dyn*. doi:10.1007/s00382-01-2763-2
- Park T-W, Ho C-H, Yang S (2011) Relationship between the arctic oscillation and cold surges over East Asia. *J Clim* 24:68–83
- Peng P, Kumar A, Wang W (2009) An analysis of seasonal predictability in coupled model forecasts. *Clim Dyn* 36:637–648
- Saha S et al (2014) The NCEP climate forecast system version 2. *J Clim* 27:2185–2208
- Shi N (1996) Features of the East Asian winter monsoon intensity on multiple time scale in recent 40 years and their relation to climate (in Chinese). *Quat J Appl Meteor* 7:175–182
- Smith TM, Reynolds RW, Peterson TC, Lawrimore J (2008) Improvements to NOAA’s historical merged land–ocean surface temperature analysis (1880–2006). *J Clim* 21:2283–2296
- Sohn S-J, Tam C-Y, Park C-K (2011) Leading modes of East Asia winter climate variability and their predictability: an assessment of the APCC multi-model ensemble. *J Meteorol Soc Jpn* 89:455–474
- Son H-Y, Park J-Y, Kug J-S, Yoo J, Kim C-H (2013) Winter precipitation variability over Korean Peninsula associated with ENSO. *Clim Dyn* 42:3171–3186

- Sung M-K, Lim G-H, Kwon W-T, Boo K-O, Kug J-S (2009) Short-term variation of Eurasian pattern and its relation to winter weather over East Asia. *Int J Climatol* 29:771–775
- Takaya K, Nakamura H (2005) Mechanisms of interannual amplification of the cold Siberian high. *J Atmos Sci* 62:4423–4440
- Thompson DWJ, Wallace JM (1998) The Arctic Oscillation signature in the wintertime geopotential height and temperature fields. *Geophys Res Lett* 25:1297–1300
- Trenberth KE, Hurrell J, Stepaniak D (2006) The Asian Monsoon: global perspectives. In: Wang B (ed) *The Asian monsoon*. Springer, Berlin, pp 67–87
- Walker GT, Bliss EW (1932) *World Weather V*. Mem R Meteorol Soc 4:53–84
- Wallace JM, Gutzler DS (1981) Teleconnections in the geopotential height field during the Northern Hemisphere winter. *Mon Weather Rev* 109:784–812
- Wang B, Wu R, Fu X (2000) Pacific-East Asian teleconnection: how does ENSO affect East Asian climate? *J Clim* 13:1517–1536
- Wang L, Chen W, Zhou W, Huang R (2009) Interannual variations of East Asian trough axis at 500 hPa and its association with the East Asian winter monsoon pathway. *J Clim* 22:600–614
- Wang L, Chen W (2010) How well do existing indices measure the strength of the East Asian winter monsoon? *Adv Atmos Sci* 27:855–870
- Wang L, Chen W (2014) An intensity index for the East Asian Winter Monsoon. *J Clim* 27:2361–2374
- Wang N, Zhang Y (2014) Evolution of Eurasian teleconnection pattern and its relationship to climate anomalies in China. *Clim Dyn* 44:1017–1028
- Wu B-Y, Wang J (2002) Winter arctic oscillation, Siberian High and East Asian winter monsoon. *Geophys Res Lett* 29:1897. doi:[10.1029/2002GL015373](https://doi.org/10.1029/2002GL015373)
- Wu B, Zhang R, D'Arrigo R (2006) Distinct modes of the East Asian winter monsoon. *Mon Weather Rev* 134:2165–2179
- Xu SY, Ji JJ (1965) The climate and weather features during the outbreak period of China's winter monsoon. *Geogr Symp* 9:85–101
- Zhang Y, Sperber K, Boyle J (1997) Climatology and interannual variation of the East Asian winter monsoon: results from the 1979–95 NCEP/NCAR reanalysis. *Mon Weather Rev* 125:2605–2619